European Radiology (2019) 29:2226–2232
https://doi.org/10.1007/s00330-018-5844-x

COMPUTED TOMOGRAPHY

Dual-energy CT in early acute pancreatitis: improved detection using iodine quantification

Simon S. Martin[1,2] · Franziska Trapp[1] · Julian L. Wichmann[1] · Moritz H. Albrecht[1] · Lukas Lenga[1] · James Durden[2] · Christian Booz[1] · Thomas J. Vogl[1] · Tommaso D'Angelo[1,3]

Received: 29 July 2018 / Revised: 19 September 2018 / Accepted: 19 October 2018 / Published online: 28 November 2018

Abstract

Objectives To evaluate the diagnostic performance of a dual-energy computed tomography (DECT)-based technique using iodine quantification and fat fraction analysis for the diagnosis of early acute pancreatitis

Methods In this retrospective study, 45 patients (35 men and 10 women; mean age, 54.9 ± 14.0 years) with early acute pancreatitis were included. Serum lipase levels and follow-up examinations served as the reference standard. A matched control group ($n = 45$) was assembled for evaluation of material decomposition values of normal pancreatic parenchyma. Three blinded radiologists independently interpreted all cases on conventional grayscale DECT series. In addition, readers re-evaluated all cases by manually performing region-of-interest (ROI) measurements on pancreatic-phase DECT material density images of the head, body, and tail of each patient's pancreas. Receiver operating characteristic (ROC) curve analysis was performed to estimate the optimal threshold for discriminating between inflammatory and normal pancreas parenchyma.

Results DECT-based iodine density values showed significant differences between inflammatory (1.8 ± 0.3 mg/mL) and normal pancreatic parenchyma (2.7 ± 0.7 mg/mL) ($p \leq 0.01$). Fat fraction measurements showed no significant differences ($p = 0.08$). The optimal iodine density threshold for the diagnosis of acute pancreatitis was 2.1 mg/mL with a sensitivity of 96% and specificity of 77%. Iodine quantification revealed an area under the curve (AUC) of 0.86, significantly higher compared to standard image evaluation of the radiologists (AUC, 0.80; sensitivity, 78%; specificity, 82%) ($p < 0.01$).

Conclusion DECT using iodine quantification allows for diagnosis of early acute pancreatitis with higher sensitivity compared to standard image evaluation.

Key Points

- *Iodine density values showed significant differences between inflammatory and normal pancreatic parenchyma.*
- *DECT using iodine quantification allows for diagnosis of early acute pancreatitis.*
- *An iodine density of ≤ 2.1 mg/mL optimizes the diagnosis of acute pancreatitis.*

Keywords Multidetector computed tomography · Pancreas · Pancreatitis · Iodine · Diagnostic imaging

✉ Julian L. Wichmann
docwichmann@gmail.com

[1] Division of Experimental and Translational Imaging, Department of Diagnostic and Interventional Radiology, University Hospital Frankfurt, Theodor-Stern-Kai 7, 60590 Frankfurt, Germany

[2] Department of Radiology and Radiological Science, Medical University of South Carolina, Charleston, SC, USA

[3] Section of Radiological Sciences, Department of Biomedical Sciences and Morphological and Functional Imaging, Policlinico G. Martino—University Hospital Messina, Messina, Italy

Abbreviations

AUC	Area under the curve
CT	Computed tomography
DECT	Dual-energy computed tomography
ROC	Receiver operating characteristics
ROI	Region of interest

Introduction

Computed tomography (CT) is an established imaging technique for the diagnosis of acute pancreatitis [1, 2]. Moreover, contrast-enhanced CT enables assessment of disease severity

as the inflammatory process can remain localized in the pancreas or spread to regional tissues and involve remote organ systems [3, 4]. Determining the severity of the disease is crucial for predicting clinical complications since severe pancreatitis, which is characterized by a protracted clinical course and multiorgan failure, occurs in 20–30% of all patients with acute pancreatitis [2]. Therefore, early staging is essential in these subjects to provide therapeutic intervention and prevent irreversible organ damage. However, while severe pancreatitis may be accurately assessed using CT, the detection or dismissal of early acute pancreatitis can be challenging since peripancreatic inflammation may not be apparent in early or mild acute pancreatitis [2–4].

Dual-energy CT (DECT) uses the information of two X-ray beam energies and the corresponding differences of absorption characteristics to perform material decomposition analysis [5]. This approach can provide accurate blood supply measurements of different tissues [6]. Several prior studies have examined DECT material decomposition analysis for tumor characterization and evaluation of tumor response [7–9]. Moreover, Yin et al investigated this technique in the field of pancreatic imaging and reported an improved diagnostic performance for the differentiation between mass-forming chronic pancreatitis and pancreatic ductal adenocarcinoma [10]. However, the value of DECT material decomposition analysis in the context of early acute pancreatitis remains unknown.

Therefore, the purpose of this study was to investigate the diagnostic performance of contrast-enhanced DECT with material decomposition analysis using iodine quantification and fat fraction analysis for the diagnosis of early acute pancreatitis.

Material and methods

Study population

This retrospective, single-center study was approved by our institutional review board, and a waiver for written informed consent was obtained. We reviewed our institutional databases to identify patients with clinically suspected early acute pancreatitis who had undergone DECT examinations on the same dual-source DECT scanner (SOMATOM Force, Siemens Healthineers) between October 2015 and January 2018. According to the revised Atlanta classification of acute pancreatitis, only patients with abdominal pain suggestive of pancreatitis (acute onset of a severe, persistent pain located in the upper abdomen and often radiating to the back) and elevated serum lipase levels three or more times than normal were included [11, 12].

Exclusion criteria were examinations with no adequate reference standard ($n = 2$) (see "Reference standard" section for details) as well as those with deviations from the standard contrast media injection protocol ($n = 5$). Further exclusion criteria were patients younger than 18 years ($n = 2$), patients with known chronic or recurrent pancreatitis ($n = 16$), and CT examinations performed after the first week of onset of disease ($n = 38$) according to the general definition of early acute pancreatitis [11]. None of the subjects had a history of primary malignancy or underwent endoscopic retrograde cholangiopancreatography (ERCP) prior to onset of the symptoms.

Our final study cohort consisted of 45 patients (mean age, 54.9 ± 14.0 years; range, 18–95 years) including 10 women (mean age, 51.4 ± 19.6 years; range, 20–78 years) and 35 men (mean age, 55.9 ± 18.7 years; range, 18–95 years) (Table 1). A control group of 45 subsequent patients (mean age, 54.5 ± 15.2; range, 21–82 years) without a history or diagnosis of pancreatic inflammation or malignancy, consisting of 10 women (mean age, 51.2 ± 18.4; range, 21–75 years) and 35 men (mean age, 55.4 ± 17.8; range, 22–82 years), was adopted to assess material density values of normal pancreatic parenchyma. All patients in the control group were scanned during the same time interval and matched by age, sex, body mass index, and clinical inclusion criteria (see "Reference standard" section for details). The flowchart of the study population enrollment was based on the recommended Standards for Reporting Diagnostic Accuracy Initiative criteria (Fig. 1).

DECT imaging technique

Abdominal DECT examinations were performed on a third-generation dual-source DECT scanner (SOMATOM Force, Siemens Healthineers). Patients were examined in supine position, and anteroposterior scout radiographs were obtained ranging from the diaphragm to the iliac crest. Image acquisition was performed in craniocaudal direction during inspiratory breath-hold. The study protocol consisted of a single pancreatic-phase acquisition in the DECT mode which

Table 1 Patients' characteristics

Characteristics	Value
Age (years)	54.9 ± 14.0*
Men (*n*)	35
Women (*n*)	10
BMI (kg/m^2)	26.2
Acute pancreatitis (*n*)	45
Grade A (*n*)	7
Grade B (*n*)	12
Grade C (*n*)	23
Grade D (*n*)	3
Grade E (*n*)	0
Control group (*n*)	45

* Data are means ± standard deviation

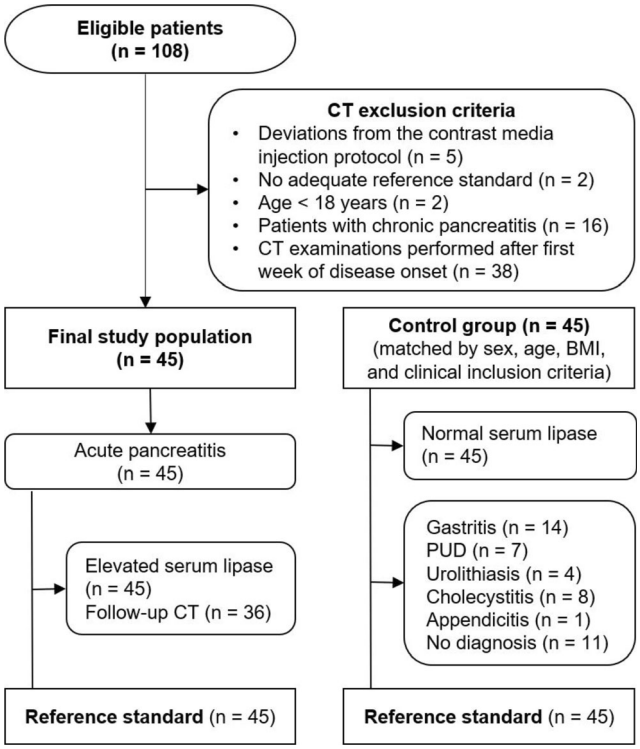

Fig. 1 Flowchart of study enrollment based on Standards for Reporting of Diagnostic Accuracy (STARD)

automatically started 50 s after the beginning of the injection of iomeprol (Imeron 350, Bracco) [13]. Contrast media was injected at a dose of 1.2 mL per kilogram body weight and at a flow rate of 3 mL/s through a superficial vein of the forearm [9, 14]. The maximum amount of contrast media was set to 120 mL. The following settings were used for DECT imaging: tube A, 90 kV and 190 mAs per rotation; tube B, Sn 150 kV with tin filter and 95 mAs per rotation; rotation time, 0.5 s; pitch, 0.6; and collimation, 2 × 192 × 0.6 mm.

The scanner generates automatically linearly blended images with a weighted factor of 0.6 (M_0.6) [15, 16]. In addition, virtual noncontrast (VNC) reconstructions were post-processed from the DECT data (Liver VNC, Siemens Healthineers), as true noncontrast scans were not acquired [17]. All image series were reconstructed with 3.0-mm section collimation in a 2.0-mm increment. DECT material decomposition images of the pancreatic-phase scan were reconstructed and analyzed on a DECT workstation (syngo.via, version VB20A, Siemens Healthineers) to calculate absolute iodine uptake (in mg/mL) and fat fraction (in %) values.

Reference standard

All study patients with early acute pancreatitis fulfilled the revised Atlanta classification and presented abdominal pain consistent with acute pancreatitis and serum lipase activity at least three times greater than the upper limit of normal [11, 12]. All CT examinations were performed during the first week of disease onset (mean, 3 days; range, 1–6 days) according to the general definition of early acute pancreatitis [11]. A subgroup of 36 patients received a control CT during the first 4 weeks (mean, 17 days; range, 7–28 days). Two expert radiologists with 31 and 7 years of experience in abdominal imaging classified all cases with acute pancreatitis by degree of disease severity (grades A–E) according to Balthazar et al [1, 2, 18]. Normal pancreatic parenchyma (grade A) was present in 7 cases. Pancreatic enlargement (grade B) was detected in 12 patients, whereas pancreatic and/or peripancreatic inflammation (grade C) was visible in 23 patients. Single peripancreatic fluid collection (grade D) was apparent in 3 cases of which 2 also showed pancreatic necrosis (≤ 30%). Two or more fluid collections (grade E) were not present in the study cohort (Table 1). In the control group, all patients presented normal serum lipase levels and did not have a tumor history or chronic pancreatitis. Patients in the control group showed the following diagnoses: gastritis ($n = 14$), gastric or duodenal ulcer ($n = 7$), kidney stone disease ($n = 4$), cholecystitis without pancreatitis ($n = 8$), and appendicitis ($n = 1$). No diagnosis was found in 11 cases.

Image analysis

Three radiologists with 5–7 years of experience in abdominal CT imaging independently evaluated all cases. Readers were blinded to the final diagnosis during this phase of assessment and were allowed to assess VNC and pancreatic-phase gray-scale images but not DECT material density images. The order in which the different cases were analyzed was randomized. During this reading session, the radiologists were asked to determine the presence or absence of pancreatitis. In a second reading session, the readers re-evaluated all cases again by manually placing region-of-interest (ROI) measurements on pancreatic-phase DECT material density images in the head, body, and tail of the pancreas in each patient. The mean value of the three measurements was used for further analysis. The readers were instructed to place the ROIs through the center of the pancreatic parenchyma to avoid margins of adjacent fat, calcifications, vessels, necrotic collections, and pancreatic cysts. In addition, normalized attenuation values were collected by subtracting VNC values from contrast-enhanced attenuation values.

Statistical analysis

The normality of data distribution was assessed using the Kolmogorov-Smirnov test. Numerical values of continuous variables were reported as mean ± standard deviation, and categorical variables were expressed as percentages. The statistically significant difference was indicated by a p value less than 0.05. The analysis of variance (ANOVA) test was used

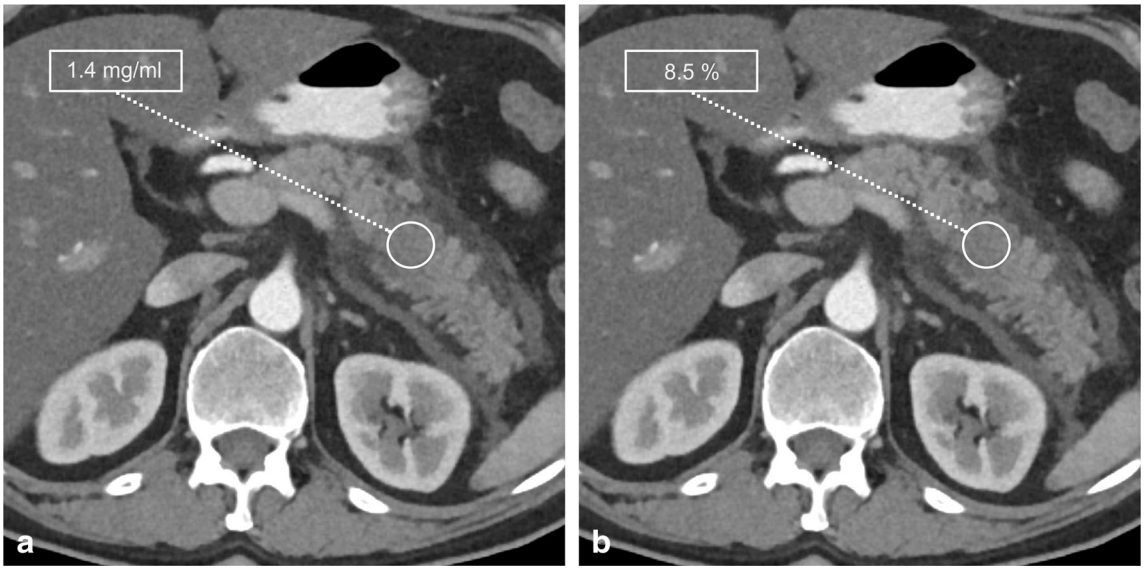

Fig. 2 DECT-based iodine quantification (**a**) and fat fraction (**b**) measurements were performed in a 62-year-old man with acute pancreatitis. In this case, peripancreatic inflammation is clearly apparent and the iodine density of 1.5 mg/mL confirms the diagnosis of acute pancreatitis as the optimal threshold for the diagnosis of acute pancreatitis is less than 2.1 mg/mL

for data showing continuous distribution, and the Wilcoxon matched-pairs test was applied in case of non-normal distribution. Serum lipase levels were used as the reference standard for all study patients. Mean values of iodine density and fat fraction were compared between inflammatory and normal pancreatic parenchyma. To establish the threshold values for material density values between normal and inflammatory pancreatic parenchyma, we adopted receiving operating characteristic (ROC) curve analysis. The diagnostic performance for the standard grayscale image evaluation of each reader was recorded including true-positive (TP), true-negative (TN), false-positive (FP), and false-negative (FN) values. The method of Delong et al was used to compare the areas under the curves (AUCs) between the iodine quantification analysis, normalized attenuation, and standard reader-based image evaluation [19]. Sensitivity and specificity values with corresponding 95% confidence intervals (CI) were determined by Youden's J statistics. To avoid overinterpretation of our diagnostic accuracy data, we performed leave-one-out cross-validation [20]. MedCalc (MedCalc Statistical Software Version 18.2, MedCalc Software bvba) was used for all statistical analyses.

Results

Mean attenuation values of inflammatory pancreatic parenchyma were 46.4 ± 12.2 Hounsfield units (HU). Normal pancreatic parenchyma showed mean attenuation values of 52.1 ± 16.1 HU with no significant differences compared to inflammatory pancreatic parenchyma ($p = 0.071$). However, normalized attenuation values revealed significant differences between inflammatory (11.3 ± 9.4 HU) and normal pancreatic parenchyma (26.1 ± 12.9 HU) ($p \leq 0.001$). Moreover, a significant difference for iodine density values was found between inflammatory (1.8 ± 0.3 mg/mL) and normal pancreas (2.7 ± 0.7 mg/mL) ($p \leq 0.001$) (Fig. 2). Mean fat fraction values showed no significant differences between patients with acute pancreatitis (12.3 ± 6.2%) and healthy patients (10.6 ± 5.1%) ($p = 0.083$) (Table 2).

The receiver operating characteristic (ROC) curve analysis demonstrated that 2.1 mg/mL was the optimal threshold to differentiate between inflammatory and normal pancreatic parenchyma by applying cross-validation (Fig. 3). This threshold showed the following results: sensitivity, 95.5% (95% CI, 90.9–98.2%), and specificity, 76.9% (95% CI, 68.0–83.4%). Analysis of normalized attenuation values yielded a sensitivity

Table 2 Results of the quantitative image analysis

	Mean attenuation (HU)	Normalized attenuation (HU)	Iodine uptake (mg/mL)	Fat fraction (%)
Acute pancreatitis*	46.4 ± 12.2	11.3 ± 9.4	1.8 ± 0.3	12.3 ± 6.2
Normal pancreas*	52.1 ± 16.1	26.1 ± 12.9	2.7 ± 0.7	10.6 ± 5.1
Optimal thresholds	–	18.8	2.1	11.1

* Data are means ± standard deviation. Normalized attenuation values were calculated by subtracting virtual noncontrast (VNC) values from contrast-enhanced attenuation values

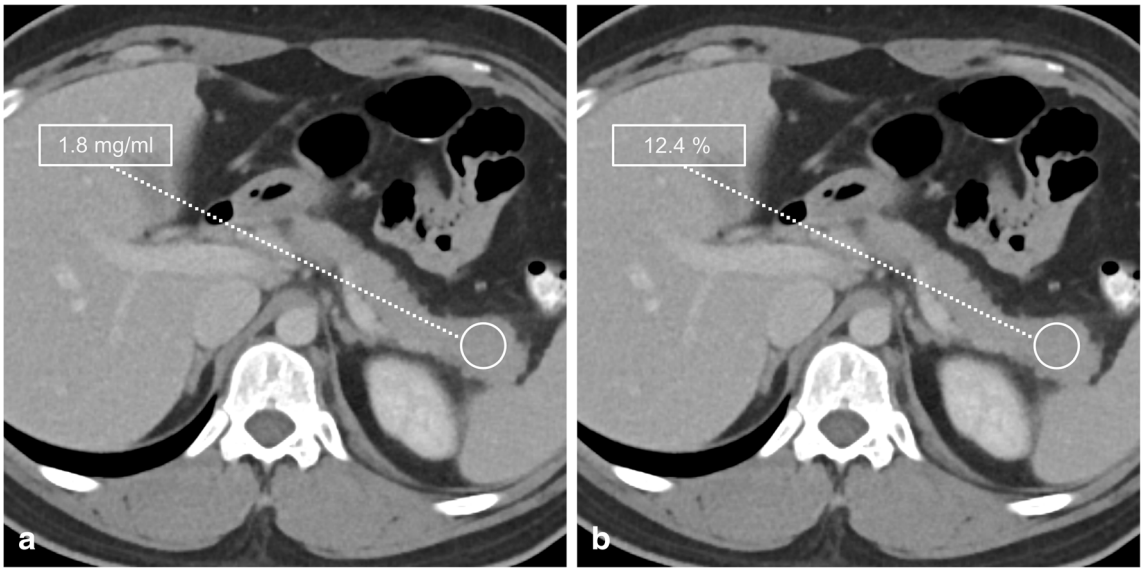

Fig. 3 DECT with material decomposition analysis was performed in a 52-year-old man with acute pancreatitis. In this case, peripancreatic inflammation is barely identifiable. However, the iodine density value of 1.8 mg/mL (**a**) indicates pancreatic inflammation. Fat fraction values (**b**) showed no significant differences between inflammatory and normal pancreatic parenchyma

of 88.1% (95% CI, 81.5–93.1%) and a specificity of 67.4% (95% CI, 58.8–75.2%) using an optimal threshold of 18.8 HU. Results of the image-based assessment revealed a sensitivity of 77.8% (95% CI, 69.8–84.5%) and a specificity of 82.2% (95% CI, 74.7–88.3%). The individual results of the image-based evaluation were the following: reader 1: TP, 33; TN, 34; FP, 11; and FN, 12; reader 2: TP, 35; TN, 38; FP, 7; and FN, 10; reader 3: TP, 37; TN, 39; FP, 6; and FN, 8. The group of false negatives ($n = 30$) entirely consisted of Balthazar grade A ($n = 19$) and grade B ($n = 11$) lesions. In contrast, the iodine quantification method correctly diagnosed 85.7% of the Balthazar grade A and 94.4% of the grade B lesions.

The AUC of the iodine quantification analysis was 0.855, significantly higher in comparison to the image-based evaluation (0.797) and attenuation-based analysis (0.834) ($p \leq 0.001$). Results of the diagnostic performance analysis are summarized in Table 3.

Discussion

The imaging-based evaluation of early acute pancreatitis relies on interpreting subtle changes which can be challenging in daily clinical routine. Our study results showed that DECT-based iodine quantification can contribute to the diagnosis of early acute pancreatitis. In this context, the threshold of 2.1 mg/mL for iodine density analysis optimizes the diagnosis of acute pancreatitis, increasing the sensitivity from 78 to 96%. However, the yielded specificity of iodine quantification was lower compared to standard image evaluation of the radiologists, and fat fraction analysis alone did not show significant benefits. On the other hand, material density analysis provided a more direct measure of iodine presence within the pancreas that resulted in a higher diagnostic accuracy in comparison to attenuation measurements.

Various DECT post-processing techniques become more widespread in the daily clinical routine, with promising results in pancreatic imaging. The reconstruction of noise-optimized virtual monoenergetic images (VMI) optimizes image quality and increases lesion delineation for pancreatic adenocarcinoma at low-kiloelectron volt levels [21, 22]. Mileto et al showed that virtual unenhanced images can replace conventional true unenhanced images for pancreatic DECT with a significant reduction of radiation dose exposure [17]. Low-tube-voltage single-phase DECT is capable of providing sufficient information for follow-up

Table 3 Results of the diagnostic performance analysis

	Normalized attenuation	Iodine uptake	Reader based
Sensitivity	88.1% (81.5–93.1%)	95.5% (90.9–98.2%)	77.8% (69.8–84.5%)
Specificity	67.4% (58.8–75.2%)	76.9% (68.0–83.4%)	82.2% (74.7–88.3%)
AUC	0.834	0.855	0.797

Data are means with corresponding 95% confidence intervals (CIs) in parentheses

AUC area under the curve

evaluation of patients with acute pancreatitis and significantly reduce radiation exposure [23].

Moreover, DECT provides quantitative information regarding tissue composition by evaluating the absorption characteristics of different materials at variable X-ray energies. This technique overcomes the limitations of attenuation-based conventional single-energy CT. Mileto et al showed that DECT material decomposition analysis showed an enhanced diagnostic accuracy for the characterization of incidental adrenal nodules compared to true unenhanced CT images [9]. A study by Tawfik et al revealed that iodine density differs significantly between healthy, inflammatory, and metastatic cervical lymph nodes [24]. Another study demonstrated that DECT in the spectral imaging mode improves diagnostic accuracy for the differentiation of mass-forming chronic pancreatitis and pancreatic ductal adenocarcinoma [10]. Iodine quantification has also shown promising results for the diagnosis of metastatic lymph nodes of other origin [25, 26]. However, experience with this iodine quantification technique in imaging of the pancreas is scarce and DECT material decomposition analysis has not yet been investigated in patients with early acute pancreatitis.

Our study results may provide additional insight into the pathophysiology of early acute pancreatitis. The iodine density of the inflammatory pancreatic parenchyma showed lower values compared to that of the normal pancreas, which could be explained by the increase in capillary permeability with subsequent fluid loss [27]. Especially in cases with no peripancreatic inflammation or pancreatic enlargement, DECT iodine quantification could potentially reduce the number of subsequent imaging studies due to the higher sensitivity. The fact that the iodine quantification method captured the majority of the Balthazar grade A and B lesions may be a potential explanation for the improved sensitivity compared to reader-based assessment. Although these grades describe only mild forms of acute pancreatitis, there is still a risk for development of severe pancreatitis. Moreover, early contrast-enhanced CT examinations may underestimate the eventual extent of pancreatic necrosis, as the impairment of pancreatic perfusion and signs of necrosis evolve over several days [1, 11, 28, 29]. In the first few days of the illness, the CT signs and patterns of pancreatic perfusion defects may be variable and difficult to detect before the area of impaired enhancement and necrosis of the pancreatic parenchyma becomes more demarcated [11]. Early detection of acute pancreatitis in these patients may be crucial in guiding these patients to follow-up examinations. Therefore, adding DECT material decomposition analysis may substantially improve the clinical workflow in patients with acute pancreatitis compared to the conventional image-based evaluation.

Some limitations of our study need to be addressed. The results of our diagnostic accuracy analysis should be considered with respect to our retrospective study design and subsequent potential case selection bias. Although we adopted leave-one-out cross-validation in our study to mitigate this limitation, a prospective study needs to be performed to validate our initial experience. Another limitation is that we investigated pancreatic-phase images, as this is the standard of care for imaging of the pancreas [13, 30]. Material density values of portal-venous-phase images could differ slightly compared to our results. In addition, the fact that we used a fixed delay for the acquisition of the pancreatic phase could have influenced our results as this technique does not take into account the cardiac output of a single patient. Finally, the implementation of a dual-source DECT scanner for material decomposition analysis may limit our study results for users of the dual-layer and rapid kilovolt-switching DECT technique. However, two studies of Pelgrim et al and Kim et al revealed that the iodine density accuracy was unaffected by the DECT system [31, 32].

In conclusion, DECT with iodine quantification allows for differentiation between normal and inflammatory pancreatic parenchyma and may substantially improve the sensitivity as a diagnostic test for the detection of early acute pancreatitis.

Funding The authors state that this work has not received any funding.

Compliance with ethical standards

Guarantor The scientific guarantor of this publication is Dr. Julian L. Wichmann.

Conflict of interest Dr. Julian L. Wichmann received speakers' fees from GE Healthcare and Siemens Healthcare. However, all data was controlled by the authors (e.g., the corresponding author) without any potential conflict of interest. The other authors of this manuscript declare no relationships with any companies, whose products or services may be related to the subject matter of the article.

Statistics and biometry No complex statistical methods were necessary for this paper.

Informed consent Written informed consent was waived by the Institutional Review Board.

Ethical approval Institutional Review Board approval was obtained.

Methodology
- Retrospective
- Diagnostic or prognostic study
- Performed at one institution

References

1. Balthazar EJ, Robinson DL, Megibow AJ, Ranson JH (1990) Acute pancreatitis: value of CT in establishing prognosis. Radiology 174: 331–336
2. Balthazar EJ (2002) Acute pancreatitis: assessment of severity with clinical and CT evaluation. Radiology 223:603–613

3. Bradley EL 3rd (1993) A clinically based classification system for acute pancreatitis: summary of the International Symposium on Acute Pancreatitis, Atlanta, Ga, September 11 through 13, 1992. Arch Surg 128:586–590
4. Mortele KJ, Wiesner W, Intriere L et al (2004) A modified CT severity index for evaluating acute pancreatitis: improved correlation with patient outcome. AJR Am J Roentgenol 183:1261–1265
5. Johnson TR, Krauss B, Sedlmair M et al (2007) Material differentiation by dual energy CT: initial experience. Eur Radiol 17:1510–1517
6. Sofue K, Itoh T, Takahashi S et al (2018) Quantification of cisplatin using a modified 3-material decomposition algorithm at third-generation dual-source dual-energy computed tomography: an experimental study. Invest Radiol 53:673–680
7. Baxa J, Matouskova T, Krakorova G et al (2016) Dual-phase dual-energy CT in patients treated with erlotinib for advanced non-small cell lung cancer: possible benefits of iodine quantification in response assessment. Eur Radiol 26:2828–2836
8. Mileto A, Marin D, Alfaro-Cordoba M et al (2014) Iodine quantification to distinguish clear cell from papillary renal cell carcinoma at dual-energy multidetector CT: a multireader diagnostic performance study. Radiology 273:813–820
9. Mileto A, Nelson RC, Marin D, Roy Choudhury K, Ho LM (2015) Dual-energy multidetector CT for the characterization of incidental adrenal nodules: diagnostic performance of contrast-enhanced material density analysis. Radiology 274:445–454
10. Yin Q, Zou X, Zai X et al (2015) Pancreatic ductal adenocarcinoma and chronic mass-forming pancreatitis: differentiation with dual-energy MDCT in spectral imaging mode. Eur J Radiol 84:2470–2476
11. Banks PA, Bollen TL, Dervenis C et al (2013) Classification of acute pancreatitis—2012: revision of the Atlanta classification and definitions by international consensus. Gut 62:102–111
12. Thoeni RF (2012) The revised Atlanta classification of acute pancreatitis: its importance for the radiologist and its effect on treatment. Radiology 262:751–764
13. Fletcher JG, Wiersema MJ, Farrell MA et al (2003) Pancreatic malignancy: value of arterial, pancreatic, and hepatic phase imaging with multi–detector row CT. Radiology 229:81–90
14. Martin SS, Pfeifer S, Wichmann JL et al (2017) Noise-optimized virtual monoenergetic dual-energy computed tomography: optimization of kiloelectron volt settings in patients with gastrointestinal stromal tumors. Abdom Radiol (NY) 42:718–726
15. Martin SS, Wichmann JL, Weyer H et al (2017) Endoleaks after endovascular aortic aneurysm repair: improved detection with noise-optimized virtual monoenergetic dual-energy CT. Eur J Radiol 94:125–132
16. Albrecht MH, Trommer J, Wichmann JL et al (2016) Comprehensive comparison of virtual monoenergetic and linearly blended reconstruction techniques in third-generation dual-source dual-energy computed tomography angiography of the thorax and abdomen. Invest Radiol 51:582–590
17. Mileto A, Mazziotti S, Gaeta M et al (2012) Pancreatic dual-source dual-energy CT: is it time to discard unenhanced imaging? Clin Radiol 67:334–339
18. Balthazar EJ, Ranson JH, Naidich DP, Megibow AJ, Caccavale R, Cooper MM (1985) Acute pancreatitis: prognostic value of CT. Radiology 156:767–772
19. DeLong ER, DeLong DM, Clarke-Pearson DL (1988) Comparing the areas under two or more correlated receiver operating characteristic curves: a nonparametric approach. Biometrics 44:837–845
20. Ochodo EA, de Haan MC, Reitsma JB, Hooft L, Bossuyt PM, Leeflang MM (2013) Overinterpretation and misreporting of diagnostic accuracy studies: evidence of "spin". Radiology 267:581–588
21. Frellesen C, Fessler F, Hardie AD et al (2015) Dual-energy CT of the pancreas: improved carcinoma-to-pancreas contrast with a noise-optimized monoenergetic reconstruction algorithm. Eur J Radiol 84:2052–2058
22. Patel BN, Thomas JV, Lockhart ME, Berland LL, Morgan DE (2013) Single-source dual-energy spectral multidetector CT of pancreatic adenocarcinoma: optimization of energy level viewing significantly increases lesion contrast. Clin Radiol 68:148–154
23. Wichmann JL, Majenka P, Beeres M et al (2014) Single-portal-phase low-tube-voltage dual-energy CT for short-term follow-up of acute pancreatitis: evaluation of CT severity index, interobserver agreement and radiation dose. Eur Radiol 24:2927–2935
24. Tawfik AM, Razek AA, Kerl JM, Nour-Eldin NE, Bauer R, Vogl TJ (2014) Comparison of dual-energy CT-derived iodine content and iodine overlay of normal, inflammatory and metastatic squamous cell carcinoma cervical lymph nodes. Eur Radiol 24:574–580
25. Rizzo S, Radice D, Femia M et al (2018) Metastatic and non-metastatic lymph nodes: quantification and different distribution of iodine uptake assessed by dual-energy CT. Eur Radiol 28:760–769
26. Li J, Fang M, Wang R et al (2018) Diagnostic accuracy of dual-energy CT-based nomograms to predict lymph node metastasis in gastric cancer. Eur Radiol. https://doi.org/10.1007/s00330-018-5483-2
27. Eibl G, Hotz HG, Faulhaber J, Kirchengast M, Buhr HJ, Foitzik T (2000) Effect of endothelin and endothelin receptor blockade on capillary permeability in experimental pancreatitis. Gut 46:390–394
28. Bollen TL, Singh VK, Maurer R et al (2012) A comparative evaluation of radiologic and clinical scoring systems in the early prediction of severity in acute pancreatitis. Am J Gastroenterol 107:612–619
29. Spanier BW, Nio Y, van der Hulst RW, Tuynman HA, Dijkgraaf MG, Bruno MJ (2010) Practice and yield of early CT scan in acute pancreatitis: a Dutch observational multicenter study. Pancreatology 10:222–228
30. Boland GW, O'Malley ME, Saez M, Fernandez-del-Castillo C, Warshaw AL, Mueller PR (1999) Pancreatic-phase versus portal vein-phase helical CT of the pancreas: optimal temporal window for evaluation of pancreatic adenocarcinoma. AJR Am J Roentgenol 172:605–608
31. Kim H, Goo JM, Kang CK, Chae KJ, Park CM (2018) Comparison of iodine density measurement among dual-energy computed tomography scanners from 3 vendors. Invest Radiol 53:321–327
32. Pelgrim GJ, van Hamersvelt RW, Willemink MJ et al (2017) Accuracy of iodine quantification using dual energy CT in latest generation dual source and dual layer CT. Eur Radiol 27:3904–3912